Available online at www.sciencedirect.com
SCIENCE DIRECT®

Ocean Engineering 33 (2006) 1589–1622

OCEAN ENGINEERING

www.elsevier.com/locate/oceaneng

Statistics of nonlinear wave crests and groups

M. Aziz Tayfun*

Civil Engineering Department, College of Engineering & Petroleum, Kuwait University, P.O. Box 5969, Safat 13060, Kuwait

Received 5 May 2005; accepted 5 October 2005
Available online 19 January 2006

Abstract

Groups of large nonlinear waves with sharper higher crests can pose hazards to ships, induce harbor resonance and cause wave-overtopping of fixed and floating structures. Past interest in wave groups has mostly been focused on the statistics and modeling of linear wave groups. Studies on nonlinear wave groups are surprisingly few, and address deep water waves only. Here, statistics of nonlinear wave crests and wave-crest groups in deep and transitional water depths are considered, using an appropriate second-order representation for crest heights and the continuous wave-envelope approach. In particular, theoretical expressions describing the statistics of nonlinear wave crests and their groups are posed in the form of a simple second-order transformation of well-known results on linear waves. Predictions from the transformation so posed compare well with nonlinear wave data gathered in the North Sea, and demonstrate that nonlinearities do affect the statistics of large wave crests and their groups significantly.
© 2005 Elsevier Ltd. All rights reserved.

Keywords: Nonlinear waves; Probability distributions; Statistics; Wave crests; Wave envelope; Wave groups; Wave steepness

1. Introduction

Statistics of linear and nonlinear wave groups are of theoretical and practical interest. Occurrences of runs of successive high waves with sharper higher crests pose

*Corresponding author. Tel.: +965 622 7814; fax: +965 481 7524.
E-mail address: tayfun@civil.kuniv.edu.kw.

0029-8018/$ - see front matter © 2005 Elsevier Ltd. All rights reserved.
doi:10.1016/j.oceaneng.2005.10.007

hazards for fixed and floating structures, and increase their vulnerability to severe damage, wave-overtopping or complete failure. Wave groups can also affect the dynamics of surf beat, and induce resonance in harbors and possibly cause the formation of unusually large or rogue waves (Stansell, 2004). Not surprisingly then, statistics of wave groups have received ample attention based on two well-known approaches: the wave-envelope approach (Rice, 1958; Longuet-Higgins, 1958) and the Markov-chain approach (Kimura, 1980). In his classic review and analysis, Longuet-Higgins (1984) shows that both approaches produce essentially similar results in comparisons with observational data. Goda (2000) also presents a succinct review of the discrete and continuous spectral versions of the Markov-chain approach. An excellent review by Masson and Chandler (1993) critically examines and compares both approaches, and discusses various modifications proposed by Vanmarcke (1975), Goda (1976), Battjes and Van Vledder (1984), and others for improving the consistency and accuracy of predicted statistics. For the continuous spectral Markov-chain approach, Stansell et al. (2002) compare accuracies of different techniques for estimating transition probabilities. Ochi and Sahinoglou (1989) and Guizhen et al. (2004) develop refinements in the wave-envelope approach.

Sharper higher wave crests ubiquitous in rough seas can significantly alter the surface geometry, fluid-flow patterns, and the attendant forces above the mean sea level. These and other wave-induced phenomena cannot be formulated adequately in terms of the statistics of wave heights and their groups. One reason for this is that unlike wave crests, wave heights do not generally appear to be affected by nonlinearities. Further, wave heights are not measured relative to a reference level whereas wave crests are, typically with respect to the local mean sea level. These are the principal justifications for studying nonlinear wave crests and their groups. But, research on nonlinear wave groups has so far been sparse, consisting of just three interesting studies. One of these is by Kriebel and Dawson (1991) based on the wave-envelope approach; the second is an experimental study by Dawson et al. (1991) on both linear and nonlinear wave groups; and, the third by Dawson et al. (1996) based on an empirical version of Kimura's (1980) discrete Markov-chain approach. All three consider deep-water waves and further approximate the original second-order narrow-band model (Tayfun, 1980, 1986) via series reversion. In this case, series reversion introduces additional errors, and leads to theoretical expressions that violate probabilistic principles. As a result, crest heights of large waves are over-predicted unrealistically in transitional water depths and also in steep storm seas in deep water (Askar and Tayfun, 1999; Forristall, 2000; Prevosto and Forristall, 2002; Wist et al., 2002). Unfortunately, most engineering interest lies in this range of large waves.

This study first explores the relative validity of a specific narrow-band type model for describing the statistics of nonlinear wave crests in deep and transitional water depths. The recent extension by Fedele and Arena (2005) of Boccotti's (2000) linear quasi-deterministic theory for the limit form of high waves to second-order unidirectional waves indicates that the model considered has general validity for large waves irrespective of any bandwidth or directional constraints. Thus, the model lends itself readily to a theoretical derivation of the statistics of nonlinear wave crests and crest groups over large waves in a fairly general context. In particular, given the proposed nonlinear model, the statistics of nonlinear crests themselves follow rather easily via a straightforward transformation of the Rayleigh law for linear wave crests. It is shown that the same nonlinear model similarly poses a simple transformation for predicting all group statistics associated with nonlinear wave crests from those appropriate to linear wave envelopes, following Longuet-Higgins' (1984) analysis and notation closely.

The crest-height definition used here and in all the references cited above refers to the global maximum in the crest segment of a wave above the local mean sea level. For linear or nonlinear waves, the statistics of such maxima are not known exactly. Previous observations (Forristall, 2000; Stansell, 2004), and also the data eventually analyzed here indicate a rather complicated bimodal structure. Observed histograms typically display an initial narrow peak over the range of relatively low waves, and a second more familiar wider peak over the mid range. At present, no theoretical or empirical model can describe this complex statistical structure even roughly. All models proposed for describing the statistics of nonlinear crest heights attempt to do so over the range of high waves beyond the second mode where the principal engineering interest lies. Thus, the particular form of the crest-height model preferred here is further justified at least on the same premise. Since 1980s, several other theoretical and semi-theoretical nonlinear crest-height models have been proposed (Marthinsen and Winterstein, 1992; Tromans and Taylor, 1998; Prevosto et al., 2000; Prevosto and Forristall, 2002; Arena and Fedele, 2002; Butler et al., 2003; Fedele, 2004). Certainly, these models all provide valuable insight into the effects of nonlinearities on wave crests. However, some are numerical or require empirical data not readily available. Others involve either intricate analytics or functional forms not amenable to practical applications or extensions to crest-group statistics.

One issue of importance that arises in the applications of all results developed here and elsewhere relates to the selection of a key parameter, often referred to as steepness parameter. In essence, the steepness parameter characterizes the nonlinearity of large waves and is closely associated with the vertical skewness of the nonlinear sea surface. The efficacy of the present model, and the accuracy of resulting statistics on wave crests and their groups depend largely on this parameter. So, various ways of specifying it are considered in detail to determine an alternative that is both simple and reasonably accurate for applications in deep and transitional water depths. Eventually, the relative validity and accuracy of all results are verified by comparisons with nonlinear wave data gathered in the North Sea.

2. Second-order random waves

2.1. General model and definitions

Consider directional waves propagating in water of locally uniform depth d. The surface fluctuations from the mean sea level are expressed as $\eta = \eta_1 + \eta_2$, where η_1 is the linear Gaussian component given by

$$\eta_1 = \sum_{j=1}^{N} a_j \cos \varepsilon_j, \tag{1}$$

with $\varepsilon_j = \vec{k}_j.\vec{x} - \omega_j t + \delta_j$, where t is time; $\vec{x}$ the horizontal position vector; $\vec{k}_j, \omega_j$ and δ_j define, respectively, the vector wave-number, radian frequency and random phase of the jth component wavelet with amplitude a_j. Wave-numbers and frequencies satisfy the dispersion relationship $\omega_j^2 = gk_j \tanh k_j d$, and $g \approx 9.81\,\mathrm{m/s^2}$. The nonlinear correction η_2 has the form

$$\eta_2 = \frac{1}{4}\sum_{i=1}^{N}\sum_{j=1}^{N} a_i a_j \{K^+ \cos(\varepsilon_i + \varepsilon_j) + K^- \cos(\varepsilon_i - \varepsilon_j)\}, \tag{2}$$

where $K^{\pm}$ represent interaction coefficients. The explicit expressions for the latter are given in Sharma and Dean (1979) and Forristall (2000).

The spectral density, say $\Omega(\omega)$, of η over the frequency ω domain will also have the form $\Omega = \Omega_1 + \Omega_2$ with Ω_1 and Ω_2 representing the spectral densities of η_1 and η_2, respectively. The ordinary moments of Ω_1 are defined by

$$m_j = \int_0^\infty \omega^j \Omega_1(\omega)\,\mathrm{d}\omega \quad (j = 0, 1, 2, \ldots). \tag{3}$$

In particular, $m_0 = \langle \eta_1^2 \rangle$, and

$$\omega_m = \frac{m_1}{m_0}, \tag{4}$$

$$\omega_0 = \sqrt{\frac{m_2}{m_0}}, \tag{5}$$

$$v = \sqrt{\frac{m_0 m_2}{m_1^2} - 1}, \tag{6}$$

define the spectral 'mean' frequency, mean zero-up-crossing frequency of η_1 and the bandwidth of Ω_1, respectively. The root-mean-square (rms) surface gradient or slope of η_1 is given by

$$\mu = \langle |\vec{\nabla}\eta_1|^2 \rangle^{1/2} = \frac{\sqrt{m_4}}{g}, \tag{7}$$

where $\vec{\nabla}$ denotes the horizontal gradient operator.

In theory, the validity of the assumed form of η requires that $\mu << 1$. The same parameter also serves as a relative measure of nonlinear corrections to η and its statistical properties (Tayfun, 1994). Evidently, η_1 is $O(\mu^0)$, whereas η_2 is $O(\mu)$. Accordingly, Ω_2 and its contributions to Ω and its moments are $O(\mu^2)$. It follows then that the spectral mean and zero-up-crossing frequencies associated with η are also given by ω_m and ω_0, correct to $O(\mu)$ and consistent with the results of

Longuet-Higgins (1964) and Huang et al. (1985). Finally, the rms surface slope of η is also μ, correct to the same order of accuracy.

2.2. Skewness coefficient and bounds

Let $\Phi_1(\vec{k})$ represent the wave-number spectral density of η_1. In the most general case, the skewness coefficient $\lambda_3 = \langle\eta^3\rangle/m_0^{3/2}$ of η can be expressed in the form (Tayfun, 1994)

$$\lambda_3 = \frac{3}{2m_0^{3/2}}\iint(K^+ + K^-)\Phi_1(\vec{k})\Phi_1(\vec{k}')\,\mathrm{d}\vec{k}\,\mathrm{d}\vec{k}' \tag{8}$$

correct to O(μ). For unidirectional waves in deep water, $K^+ = k + k' = (\omega^2 + \omega'^2)/g$ and $K^- = -|k - k'| = -|\omega^2 - \omega'^2|/g$. In this case, Eq. (8) assumes the simpler form

$$\lambda_3 = \frac{3}{2gm_0^{3/2}}(I^+ - I^-), \tag{9}$$

where

$$I^+ = \iint(\omega^2 + \omega'^2)\Omega_1(\omega)\Omega_1(\omega')\,\mathrm{d}\omega\,\mathrm{d}\omega' = 2m_0^2\omega_0^2, \tag{10}$$

$$I^- = \iint|\omega^2 - \omega'^2|\Omega_1(\omega)\Omega_1(\omega')\,\mathrm{d}\omega\,\mathrm{d}\omega', \tag{11}$$

and $0<\omega,\omega'<\infty$. The preceding expressions can be easily combined to rewrite λ_3 as (Longuet-Higgins, 1963)

$$\lambda_3 = \frac{I}{m_0^{3/2}} = \frac{6}{gm_0^{3/2}}\int_0^\infty\int_0^{\omega'}\omega^2\Omega_1(\omega)\Omega_1(\omega')\,\mathrm{d}\omega\,\mathrm{d}\omega'. \tag{12}$$

Now, note that $(\omega - \omega')^2 \leqslant |\omega^2 - \omega'^2|$ in I^-. On this basis, it can be verified that (see, e.g. Tayfun, 1986)

$$I^- \geqslant \iint(\omega - \omega')^2\Omega_1(\omega)\Omega_1(\omega')\,\mathrm{d}\omega\,\mathrm{d}\omega' = 2m_0^2\omega_m^2\nu^2. \tag{13}$$

This result and Eq. (10) can now be substituted together with $\omega_0^2 = (1+\nu^2)\omega_m^2$, $\omega_m^2 = gk_m$ and $\omega_0^2 = gk_0$ in Eq. (9) to obtain

$$\lambda_3 \leqslant 3\mu_m = 3\frac{\mu_0}{1+\nu^2}, \tag{14}$$

where

$$\mu_m = m_0^{1/2}k_m, \tag{15}$$

$$\mu_0 = \mu_m(1+\nu^2) = m_0^{1/2}k_0 \tag{16}$$

represent measures of surface slope or steepness. As $\nu \to 0$ in deep water, then $\mu_m \to \mu_0$. Thus, μ_0 corresponds to the narrow-band least-upper-bound (l.u.b.)

considered previously in Tayfun and Al-Humoud (2002) and Tayfun (2004), except for $\sqrt{2}$ that arises from the different scaling used in these references.

Proceeding further, consider I^-again and note that $|\omega^2 - \omega'^2| = (\omega + \omega')|\omega - \omega'|$. Under narrow-band conditions, $\omega + \omega' \approx 2\omega_m$. This approximation and Schwarz's inequality can now be used in Eq. (11) to obtain

$$I^- \approx 2\omega_m \iint |\omega - \omega'| \Omega_1(\omega)\Omega_1(\omega')\, \mathrm{d}\omega\, \mathrm{d}\omega' \leqslant 2\sqrt{2} m_0^2 \omega_m^2 v. \tag{17}$$

Substituting this approximation, Eq. (10) and $\omega_m^2 = gk_m$ in Eq. (10) will lead to

$$\lambda_3 \geqslant 3\mu_m(1 - v\sqrt{2} + v^2). \tag{18}$$

Thus,

$$3\mu_m(1 - v\sqrt{2} + v^2) \leqslant \lambda_3 \leqslant 3\mu_m. \tag{19}$$

Because $\mu_m = \mu_0/(1 + v^2)$, this result can also be rewritten in terms of μ_0 and v as

$$3\mu_0\left(1 - \frac{v\sqrt{2}}{1 + v^2}\right) \leqslant \lambda_3 \leqslant 3\frac{\mu_0}{1 + v^2}. \tag{20}$$

2.3. Narrow-band model

The scaled surface elevation $\hat{\eta} = \eta/m_0^{1/2}$ from the mean water level will be approximated by

$$\hat{\eta}(t) = r\cos\chi + \frac{1}{2}\mu^* r^2 \cos 2\chi, \tag{21}$$

where the leading term is the first-order zero-mean Gaussian $\hat{\eta}_1 = \eta_1/m_0^{1/2}$ *exactly*, irrespective of directional or spectral properties, and the second term represents the second-order nonlinear correction $\hat{\eta}_2 = \eta_2/m_0^{1/2}$, correct to $O(v^0)$ in general. The random function $r(t)$ represents the linear wave amplitude or envelope scaled with $m_0^{1/2}$, and is Rayleigh-distributed. The total phase $\chi(t)$ is uniformly random in $(0, 2\pi)$. In transitional depths, the dimensionless parameter μ^* is proportional to the *rms* surface slope. In deep water, $\mu^* \to \mu$, correct to $O(v^0)$.

Since $\langle\hat{\eta}\rangle = 0$ and $\langle\hat{\eta}^2\rangle = 1$, correct to $O(\mu^*)$, the skewness coefficient of $\hat{\eta}$ is given to the same order by

$$\lambda_3 = \langle\hat{\eta}^3\rangle = 3\mu^*. \tag{22}$$

Thus, Eq. (21) can be rewritten in the equivalent form

$$\hat{\eta} = r\cos\chi + \frac{1}{6}\lambda_3 r^2 \cos 2\chi. \tag{23}$$

3. Statistics of nonlinear crest heights and groups

3.1. Crest heights

The probability density function (pdf) and exceedance probability distribution (epd) of r are given, respectively, by

$$p_r(r) = r\exp(-r^2/2), \tag{24}$$

$$E_r(r) = \exp(-r^2/2), \tag{25}$$

where $r \geqslant 0$ by definition. Nonlinear crests and troughs, say, y and y^- scaled with $m_0^{1/2}$ would then follow from Eqs. (21) and (23) with $\chi = 0$ as

$$y = r + \frac{1}{2}\mu^* r^2 = r + \frac{1}{6}\lambda_3 r^2, \tag{26}$$

$$y^- = r - \frac{1}{2}\mu^* r^2 = r - \frac{1}{6}\lambda_3 r^2. \tag{27}$$

It should be noted that the expressions recently derived by Fedele and Arena (2005) for describing crests and troughs of unidirectional waves in deep water are identical to the preceding equations. Apparently, Fedele and Arena did not recognize this, and presented their results (cf. Eqs. (13) and (14) in Fedele and Arena, 2005) in terms of a double integral identical to λ_3 in Eq. (9). In other words, Eqs. (26) and (27) are valid for unidirectional seas in deep water for $r >> 1$ irrespective of any bandwidth constraints. Further, the Fedele–Arena derivation can easily be generalized to directional seas in deep or transitional water depths to show that the same expressions have in fact general validity for $r >> 1$, with λ_3 given by Eq. (8). The comparisons of various theoretical results based on Eq. (26) with oceanic data will later show that the crest-height model considered here is indeed valid under general conditions for $r > 1.25$ approximately.

The pdf and epd of y can be expressed as

$$p(y) = \frac{p_r(r)}{1+\mu^* r}, \quad y = r\left(1 + \frac{1}{2}\mu^* r\right), \tag{28}$$

$$E(y) = E_r(r), \quad y = r\left(1 + \frac{1}{2}\mu^* r\right). \tag{29}$$

Further, the conditional mean $y_{1/n}$ of y, given that $y > y_n = E^{-1}(1/n)$ is of the form

$$y_{1/n} = r_{1/n} + \mu^*[1 + \ln(n)] \quad (n = 1, 2, \ldots), \tag{30}$$

where

$$r_{1/n} = \sqrt{2\ln(n)} + n\sqrt{\frac{\pi}{2}}\operatorname{erfc}\{\sqrt{\ln(n)}\} \tag{31}$$

represents the conditional mean of r, given that $r > r_n = E_r^{-1}(1/n)$, and erfc is the complementary error function (Abramowitz and Stegun, 1968). As an example of practical interest, consider the case where $n = 3$. For this case, Eqs. (30) and (31) lead to $y_{1/3}/r_{1/3} = 1 + 1.0483\mu^*$. This result then suggests that when $\mu^* \approx 0.08$–0.10 as a typical range in stormy seas, nonlinearities amplify 'significant' crest heights by about 8–10% above the expected linear values.

3.2. Crest groups

Viewed as functions of time t, Eqs. (26) and (27) describe the upper and lower envelopes of $\hat{\eta}$, respectively. Of present interest is the upper envelope and, in specific, its number of up-crossings of a given level y per unit time, more simply referred to as the level or threshold up-crossing rate. It has the general form (Rice, 1958):

$$N_y = \int_0^\infty p(y, \dot{y})\dot{y}\, \mathrm{d}\dot{y} = \int_0^\infty p(y)p(\dot{y}|y)\dot{y}\, \mathrm{d}\dot{y}, \tag{32}$$

where $\dot{y}$ is the time derivative of y, $p(y, \dot{y})$ represents the joint pdf of y and $\dot{y}$, and $p(y|\dot{y})$ is the conditional pdf of y, given $\dot{y}$. The latter follows from Eq. (26) as

$$\dot{y} = \dot{r}(1 + \mu^* r). \tag{33}$$

Now, let $p_{\dot{r}}(\dot{r})$ and $p_{\dot{r}/r}(\dot{r}|r)$ represent, respectively, the marginal and conditional pdf of $\dot{r}$, given r. Since r and $\dot{r}$ are statistically independent, $p_{\dot{r}/r}(\dot{r}|r) = p_{\dot{r}}(\dot{r})$. On this basis, it is easily verified that

$$p(y)p(\dot{y}|y)\dot{y}\, \mathrm{d}\dot{y} = \frac{p_r(r)}{1 + \mu^* r} p_{\dot{r}/r}(\dot{r}|r)\dot{r}(1 + \mu^* r)\, \mathrm{d}\dot{r} = p_r(r)p_{\dot{r}}(\dot{r})\dot{r}\, \mathrm{d}\dot{r}, \tag{34}$$

where (see, e.g. Rice, 1958; Longuet-Higgins, 1984)

$$p_{\dot{r}}(\dot{r}) = \frac{1}{v\omega_m\sqrt{2\pi}} \exp\left(-\frac{\dot{r}^2}{2v^2\omega_m^2}\right), \quad -\infty < \dot{r} < \infty. \tag{35}$$

Substituting Eqs. (34) and (35) in Eq. (32) will yield

$$N_y = N_r = \frac{v\omega_m}{\sqrt{2\pi}} p_r(r), \quad y = r\left(1 + \frac{1}{2}\mu^* r\right), \tag{36}$$

where N_r represents the up-crossings rate of level r by the linear envelope, as in Longuet-Higgins (1984). As a principal and yet strikingly simple result, Eq. (36) suggests that the up-crossing rate N_y of level $y = r(1 + \mu^* r/2)$ by the nonlinear envelope is given by the up-crossing rate N_r of level r by the linear envelope. It is then immediate from this and Longuet-Higgins (1984) that the mean number G_y of waves between groups with crest heights higher than y is given by

$$G_y = G_r = \frac{\omega_0}{v\omega_m\sqrt{2\pi}} \frac{1}{p_r(r)}, \quad y = r\left(1 + \frac{1}{2}\mu^* r\right), \tag{37}$$

where ω_0 represents the mean zero-up-crossing frequency of the nonlinear envelope, correct to $\mathrm{O}(\mu^*)$, as was previously mentioned in Section 2.1. Finally, the average number H_y of waves in a group with crest heights above y can be expressed as

$$H_y = G_r E_r(r) = \frac{\omega_0}{v\omega_m\sqrt{2\pi}} \frac{1}{r}, \quad y = r\left(1 + \frac{1}{2}\mu^* r\right). \tag{38}$$

As $\mu^* \to 0$, $y \to r$, and the preceding results simply converge to the statistics appropriate to linear waves. Since $\omega_0 = (1 + v^2)^{1/2}\omega_m$ in general, they can also be expressed all in terms of the bandwidth parameter v, as in Longuet-Higgins (1984). This will not be done here for functional simplicity. Clearly, all results as they are given above in terms of the actual parameters v, ω_m and ω_0 apply to the upper wave envelope. So, to translate them into statistics of discrete wave-crest groups, these three parameters will have to be replaced, as in Longuet-Higgins (1984), with the values determined from the surface spectral density band-passed over frequencies within the interval $(0.5\omega_{\mathrm{p}}, 1.5\omega_{\mathrm{p}})$, where ω_{p} stands for the spectral-peak frequency.

4. Parameter μ^*

4.1. Estimating μ^* from observed λ_3

Assume for the moment that Eq. (21) is valid, and thus Eq. (26) describes the nonlinear crest heights exactly. This presupposes that μ^* is either known or can be derived from Eq. (22), given an estimate of λ_3. In theory, this rationale appears quite sensible since λ_3 can be estimated rather easily from a wave record. In practice, however, it raises at least two immediate points of concern. First, λ_3 derived from a wave record tends to be an unstable statistic because of its sensitivity to local trends and/or the presence of an exceptionally large wave in the record. Second, estimating λ_3 from a wave record treated as a whole yields an estimate of μ^* representative of all waves whereas models of the type considered here are really appropriate to the crest heights of large waves. So, λ_3 and thus μ^* would have to be estimated from the surface time history representing relatively high waves under steady sea-state conditions. Though conceptually simple, this approach is neither practical nor predictive since it necessitates wave-by-wave analyses of wave records.

4.2. Estimating μ^* from upper bounds of λ_3

In directional deep-water waves, the skewness coefficient satisfies the condition (Longuet-Higgins, 1963)

$$0.44\frac{I}{m_0^{3/2}} \leqslant \lambda_3 \leqslant 1.01\frac{I}{m_0^{3/2}}, \tag{39}$$

where I is defined as in Eq. (12). The results in Section 2.2 can now be coupled with Eq. (39) to further improve the upper and lower bounds to λ_3, and thus to μ^* in the form

$$\mu_{\mathrm{lb}} \leqslant \mu^* = \frac{\lambda_3}{3} \leqslant \mu_{\mathrm{ub}}, \tag{40}$$

where

$$\mu_{\mathrm{lb}} = 0.44\mu_m(1 - v\sqrt{2} + v^2), \quad \mu_{\mathrm{ub}} = 1.01\mu_m \approx \mu_m. \tag{41}$$

As $v \to 0$, $\mu_m \to \mu_0$, and Eq. (40) leads to the narrow-band l.u.b. $\lambda_3 \approx 3\mu_0$, as mentioned previously. If μ^* is replaced by μ_0 in Eq. (26), then the resulting distribution E and conditional mean $y_{1/n}$ tend to describe the statistics of large wave crests in storm seas reasonably well, in particular, locally over relatively short periods of time, say, approximately during 1 h of observations coincident with the peak storm conditions (Tayfun and Al-Humoud, 2002; Tayfun, 2004). In the more general case, the upper bound is given by $\lambda_3 \approx 3\mu_m$, and setting $\mu^* = \mu_{\mathrm{ub}} \approx \mu_m$ renders the present model identical with the original narrow-band model (Tayfun 1980, 1886; Askar and Tayfun, 1999). In describing wave crests over relatively long periods of time, say over several hours under steady sea-state conditions, setting $\mu^* \approx \mu_m$ tends to yield predictions that compare more closely with the observed statistics, as will be shown later.

4.3. Estimating μ^* from Forristall's Weibull model

In the most general case of waves at transitional water depths, the functional form of the skewness coefficient in Eq. (8) presents complexities (Forristall, 2000) in that it does not appear amenable to further simplifications nor does it allow any upper or lower bound considerations as easily as is possible in deep water. Thus, as an alternate approach for estimating μ^*, consider the third moment of y, which follows to $O(\mu^*)$ from Eq. (26) as

$$\langle y^3 \rangle = 3\sqrt{\frac{\pi}{2}} + 12\mu^*. \tag{42}$$

Thus, given an estimate of $\langle y^3 \rangle$, this equation can be solved to obtain

$$\mu^* = \frac{1}{12}\left(\langle y^3 \rangle - 3\sqrt{\frac{\pi}{2}}\right). \tag{43}$$

Clearly, $\langle y^3 \rangle$ can be estimated from a wave record directly, restricting attention to crest heights over high waves. The shortcoming of this is that the resulting model can no longer be regarded as a predictive model as it relies on the observed crests themselves.

A more practical approach is to appeal to one of several formulations proposed for the distribution of crest heights in transitional water depths. These include the models in Marthinsen and Winterstein (1992), Prevosto et al. (2000), Forristall (2000), and Prevosto and Forristall (2002). For the purpose of estimating $\langle y^3 \rangle$ in directional seas, the most general of these is Forristall's two-parameter Weibull distribution fitted to simulated second-order wave crests in unidirectional (2D) and directional (3D) seas. Forristall's Weibull pdf and epd for crest heights scaled with $m_0^{1/2}$ are given in the present notation by

$$p(y) = \frac{\beta}{4\alpha}\left(\frac{y}{4\alpha}\right)^{\beta-1} \exp\left[-\left(\frac{y}{4\alpha}\right)^{\beta}\right], \tag{44}$$

$$E(y) = \exp\left[-\left(\frac{y}{4\alpha}\right)^{\beta}\right], \tag{45}$$

where α and β represent parameters. As $\alpha \to 1/2\sqrt{2}$ and $\beta \to 2$, the Weibull model leads to the Rayleigh limits in Eqs. (24) and (25).

The conditional mean $y_{1/n}$ associated with the Weibull model can be expressed as

$$y_{1/n} = 4\alpha\left\{(\ln n)^{1/\beta} + n\frac{1}{\beta}\Gamma\left(\frac{1}{\beta}\right)\left[1 - \mathrm{P}\left(\frac{1}{\beta}, \ln n\right)\right]\right\}, \tag{46}$$

where $n = 1,2,\ldots,$ and Γ and P stand for the gamma and incomplete gamma functions, respectively (Abramowitz and Stegun, 1968). Further, the third-order moment of y as a Weibull-distributed variable is given by

$$\langle y^3 \rangle = \frac{3(4\alpha)^3}{\beta}\Gamma\left(\frac{3}{\beta}\right). \tag{47}$$

Upon substitution in Eq. (43), this yields

$$\mu^* = 16\frac{\alpha^3}{\beta}\Gamma\left(\frac{3}{\beta}\right) - \frac{1}{4}\sqrt{\frac{\pi}{2}} \tag{48}$$

and thus allows Forristall's Weibull fit to be coupled with the present model.

Because Forristall's Weibull model is empirical and not based on an explicit functional representation of the sea surface or wave crests, it does not readily lend itself to the derivation of any statistics on wave-crest groups. But, coupling it with the present crest-height model in the manner described does. Further, preliminary comparisons with observational data showed that the theoretical predictions based on μ^* estimated from $\langle y^3 \rangle$ of Forristall's Weibull model describe the crest heights of high waves surprisingly well. In theory, μ^* can also be estimated using the lower- or higher-order moments of y. However, the lower-order moments yield smaller μ^* values, and thus lead to theoretical predictions that underestimate the observed crest heights noticeably. And, the higher-order moments yield much larger μ^* values that overestimate the observed trends significantly.

4.4. *Weibull parameters α and β*

Forristall's Weibull fit to 2D simulations lead to

$$\alpha_2 = \frac{1}{2\sqrt{2}} + 0.2892S_1 + 0.1060\,Ur, \tag{49}$$

$$\beta_2 = 2 - 2.1597S_1 + 0.0968\,Ur^2 \tag{50}$$

and, for 3D simulations,

$$\alpha_3 = \frac{1}{2\sqrt{2}} + 0.2568S_1 + 0.0800\,Ur, \tag{51}$$

$$\beta_3 = 2 - 1.7912S_1 - 0.5302\,Ur + 0.284\,Ur^2, \tag{52}$$

where S_1 and Ur are steepness and Ursell parameters. In the present notation,

$$S_1 = \frac{2}{\pi}\frac{m_0^{1/2}}{d}q_m, \tag{53}$$

$$Ur = \frac{4}{q_1^2}\frac{m_0^{1/2}}{d}, \tag{54}$$

where $q_m = k_m d = \omega_m^2 d/g$ and $q_1 = k_1 d$ such that

$$q_m = q_1 \tanh q_1. \tag{55}$$

Forristall's results suggest that 2D simulations describe the observed data better in deep water, whereas 3D simulations do so in shallow water where the skewness coefficient λ_3 becomes larger than the values predicted by the 2D random-wave model. On this basis, the parameter μ^* sought for modeling wave crests correctly corresponds to the larger of the two values that follow from Eq. (48) with (α_2, β_2) and (α_3, β_3), respectively. Hereafter, these will be differentiated and referred to as μ_{F2} and μ_{F3}, respectively.

4.5. Range of validity

The second-order deterministic Stokes representation is valid at transitional depths if the Ursell parameter satisfies the condition (Peregrine, 1972)

$$Ur = \frac{H}{q^2 d} \leqslant 2, \tag{56}$$

where H represents wave height and $q = kd$. Dean and Dalrymple (1998) further show that the more stringent condition $U_r \leqslant \frac{2}{3}$ has to be satisfied to exclude the occurrence of anomalous bumps or negative maxima in wave troughs. This rationale does not apply to irregular waves, and need not be considered here. However, wave heights tend to be bounded by an upper limit (Miche, 1944). An equivalent expression for this limit is given by

$$\frac{H}{d} \leqslant \frac{2\pi}{7}\frac{\tanh q}{q}. \tag{57}$$

Now, if the maximum ratio H/d given by the right-hand side equality in the preceding expression is substituted in Eq. (56), then both conditions will be satisfied for values of $q \geqslant q_{\min}$, where

$$q_{\min}^3 = \frac{\pi}{7}\tanh q_{\min} \tag{58}$$

with the solution $q_{\min} = 0.6305$.

The preceding results do not generally apply to directionally spread irregular waves. However, they should have some bearing on long-crested irregular waves if H and k are interpreted as zero-up-crossing properties. For instance, if $H \approx 2m_0^{1/2} r$ is substituted in Eq. (57), it can be rearranged and expressed in the equivalent form

$$r \leqslant r_{\max} = \frac{d}{m_0^{1/2}} q_{\min}^2 \approx 0.4 \frac{d}{m_0^{1/2}}. \tag{59}$$

Theoretically, this condition restricts the range of validity of r as a Rayleigh-distributed variable with no upper bound. For example, setting $d/m_0^{1/2} = 10$ leads to the restricted range $0 < r \leqslant r_{\max} \approx 4$. The probability that $r > 4$ is not exactly 0, but follows from Eq. (25) as $E_r(4) = 3.4 \times 10^{-4}$. If larger wave heights at lower probabilities of occurrence than this are of concern, then the Rayleigh law may have to be modified to satisfy the Miche condition. For most applications where $d/m_0^{1/2} > 10$, the indicated probability levels are sufficiently low to have any significant effect on the results derived from the Rayleigh approximation. The experimental results of Doering and Donelan (1993) on irregular waves shoaling on seabed slopes as large as $\frac{1}{5}$ lend strong support to this rationale. Thus, the theoretical approximations considered above should be valid for $q_1 > 0.630$ or, equivalently, when $q_m > 0.352$ at transitional water depths, provided that $d/m_0^{1/2} > 10$ approximately.

Forristall's definition of S_1 is based on depth-dependent parameters except for q_m. Evidently, the latter can be expressed in terms of q_1 so that the Miche condition on S_1 becomes

$$S_1 \leqslant \max S_1 = \tfrac{1}{7} \tanh^2 q_1. \tag{60}$$

In deep water where $q_1 \to \infty, \max S_1 \to \frac{1}{7} \approx 0.1428$ as an upper bound, well-known as the Stokes limiting steepness. As $q_1 \to q_{\min}$ in shallower depths, $\max S_1 \to 0.0445$ as a lower bound. The corresponding range of the Ursell parameter is then given by $0 < Ur < 10.062\ m_0^{1/2}/d$. Consequently, Forristall's Weibull model satisfies the Ursell and Miche conditions both, if

$$0.0445 < S_1 < \frac{1}{7}, \tag{61}$$

$$0 < Ur < 10.062 \frac{m_0^{1/2}}{d}. \tag{62}$$

Assuming further that $d/m_0^{1/2} > 10$, the preceding results lead to the following approximate bounds on the allowable values of α and β:

$$\frac{1}{2\sqrt{2}} < \alpha_2 < 0.4731, \quad 1.6915 < \beta_2 < 2, \tag{63}$$

$$\frac{1}{2\sqrt{2}} < \alpha_3 < 0.4455, \quad 1.6743 < \beta_3 < 2. \tag{64}$$

The values of the parameters μ_{F2} and μ_{F3} that follow from these and Eq. (48) are shown in Fig. 1 for various values of $d/m_0^{1/2}$. It may be noticed that for $d/m_0^{1/2}$ given, μ_{F3} derived from 3D parameters is slightly larger for $q_m \leqslant q^*$, where q^* is indicated with hollow circular points in the figure. For $q_m > q^*$, 2D parameters yield the larger μ_{F2} values in general. As $d/m_0^{1/2}$ increases from 10 to 50, q^* decreases from 1.108 to 0.856, respectively.

The present upper bound can also be rewritten as $\mu_m = (m_0^{1/2}/d)q_m$. This then permits a comparison between μ_m and μ_{F2}, as is shown in Fig. 2. It is seen that for

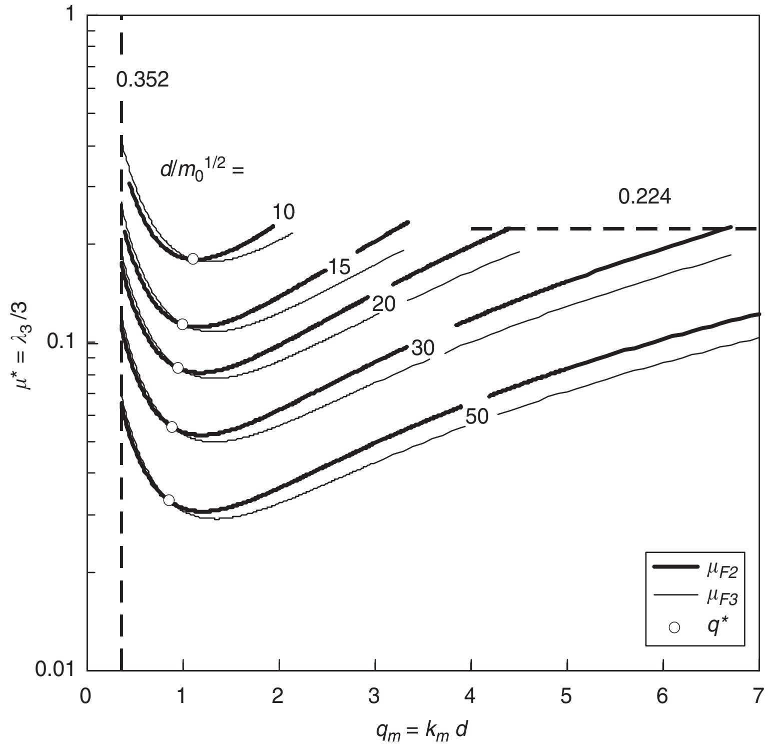

Fig. 1. Steepness parameter μ_{F2} and μ_{F3} versus q_m for various values of $d/m_0^{1/2}$.

$m_0^{1/2}/d \geqslant 20$, μ_m still serves as an upper bound to μ^* in transitional depths, provided that $q_m \geqslant \mathrm{q}^\dagger$, where $q^\dagger$ decreases from 1.90 to 1.62 as the ratio $m_0^{1/2}/d$ increases from 20 to 50.

5. Kriebel–Dawson model

5.1. Probability structure

In Kriebel and Dawson (1991, 1993), the probability structure of y is derived from a reversion of Eq. (26) to express r as a function of y in the form

$$r = y - \frac{1}{2}\mu^* y^2. \tag{65}$$

Using this in standard probability transformations and retaining only terms to O(μ^*) in algebraic expressions will give the pdf and epd of y in the present notation as

$$p(y) = y\left(1 - \frac{3}{2}\mu^* y\right)\exp\left[-\frac{1}{2}y^2(1 - \mu^* y)\right], \tag{66}$$

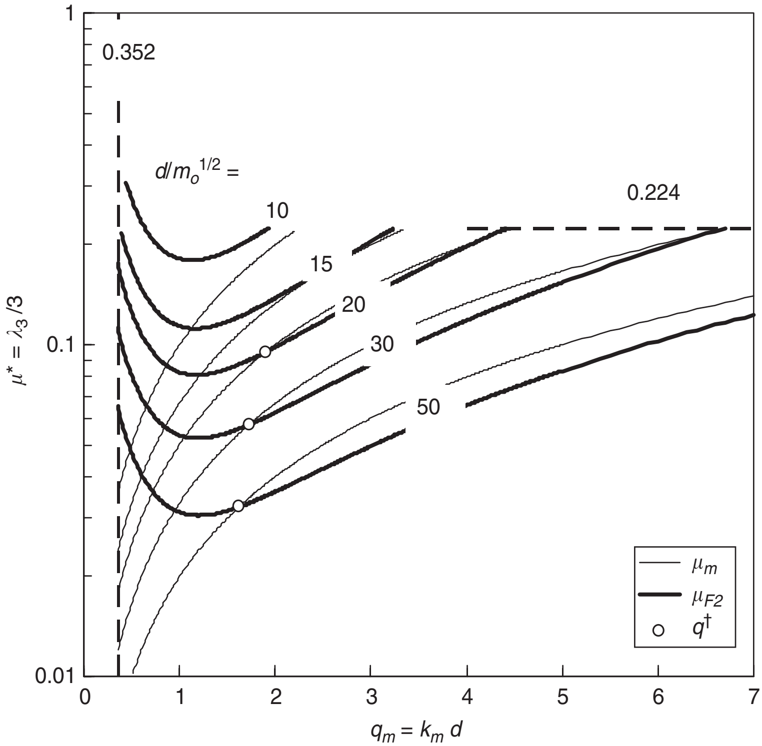

Fig. 2. Same as Fig. 1 but for μ_m and μ_{F2}.

$$E(y) = \exp\left[-\frac{1}{2}y^2(1-\mu^* y)\right]. \tag{67}$$

Evidently, p is not normalized as a proper pdf. It also becomes negative for $y > \frac{2}{3}\mu^*$. In theory, $E \leqslant 1$ and it must monotonously decrease to 0 as $y \to \infty$. In fact, it increases for $y > \frac{2}{3}\mu^*$, and exceeds 1 eventually. At least one obvious drawback of all this is that ordinary and conditional moments of y such as $y_{1/n}$ cannot be derived from either p or E.

5.2. Group statistics

The principal statistics on wave-crest groups that follow from the Kriebel–Dawson approximations can be expressed in present notation as

$$Ny = \frac{v\omega_m}{\sqrt{2\pi}} \frac{p(y)}{1-\mu^* y}, \tag{68}$$

$$G_y = \frac{\omega_0}{v\omega_m\sqrt{2\pi}} \frac{(1-\mu^* y)}{y(1-3\mu^* y/2)} E(y), \tag{69}$$

$$H_y = \frac{\omega_0}{v\omega_m\sqrt{2\pi}} \frac{1-\mu^* y}{y(1-3\mu^* y/2)}. \tag{70}$$

The preceding expressions are identical to Eqs. (25), (26) and (31) in Kriebel and Dawson (1991), except for $\omega_0/\sqrt{2\pi}$ included in Eqs. (69) and (70) for later comparison with the present results.

5.3. Parameter μ^*

For narrow-band long-crested waves at transitional depths, the steepness parameter can be expressed, correct to $O(v^0)$, in the form

$$\mu^* = \mu_1 f_{\mathrm{d}}, \tag{71}$$

where $\mu_1 = m_0^{1/2} k_1$, k_1 relates to the spectral mean frequency ω_m via dispersion Eq. (55) as before, and $f_{\mathrm{d}} = D_1 + D_2$ represents a dimensionless depth function in which

$$D_1 = \frac{1}{2} \frac{4n-1}{n^2 \tanh q_1 - q_1}, \tag{72}$$

$$D_2 = \frac{\cosh q_1 (2 + \cosh 2q_1)}{2 \sinh^3 q_1} \tag{73}$$

with $n = [1 + (2q_1/\sinh 2q_1)]/2$. The factors D_1 and D_2 arise from the frequency-difference and frequency-sum terms, viz. $K^-$and K^+ in Eq. (2), as $v \to 0$. These were derived originally by Marthinsen and Winterstein (1992). In a similar and somewhat more general context, they are defined in Prevosto et al. (2000) as $2c_{\mathrm{diff}}$ and $2c_{\mathrm{sum}}$, respectively. Although their functional forms differ in appearance from one another as given in these references and here, they reduce with some straightforward algebra exactly to the somewhat simpler and more familiar forms given above.

The steepness parameter in Kriebel and Dawson (1993) is defined as

$$\mu^* = \mu_{\mathrm{KD}} = \mu_m f_2, \tag{74}$$

where $f_2 = D_2 + D_3$, with D_2 as defined before, and

$$D_3 = -\frac{1}{\sinh 2q_1}. \tag{75}$$

Clearly, f_2 is formulated in analogy with the deterministic Stokes theory (see, e.g., Dean and Dalrymple, 1993). In deep water where both q_m and q_1 become large, $f_2 \to 1$ and $\mu^* \to \mu_m$ as lower bounds. But, $f_2 > 1$ generally, and it becomes increasingly large in shallower water depths. The principal reason for this discrepancy is that the 'randomized' adaptations of the deterministic Stokes theory for periodic waves of permanent form do not always lead to physically and theoretically consistent representations of irregular waves (Tayfun, 1986; Marthinsen and Winterstein, 1992; Prevosto and Forristall, 2002). This appears to be the case for the Kriebel–Dawson model at transitional depths, and also for other models similarly proposed since early 1980s (Arhan and Plaisted, 1981; Huang et al., 1983; Arena and Fedele, 2002; Dawson, 2004). In the present case, D_1 and D_3 differ

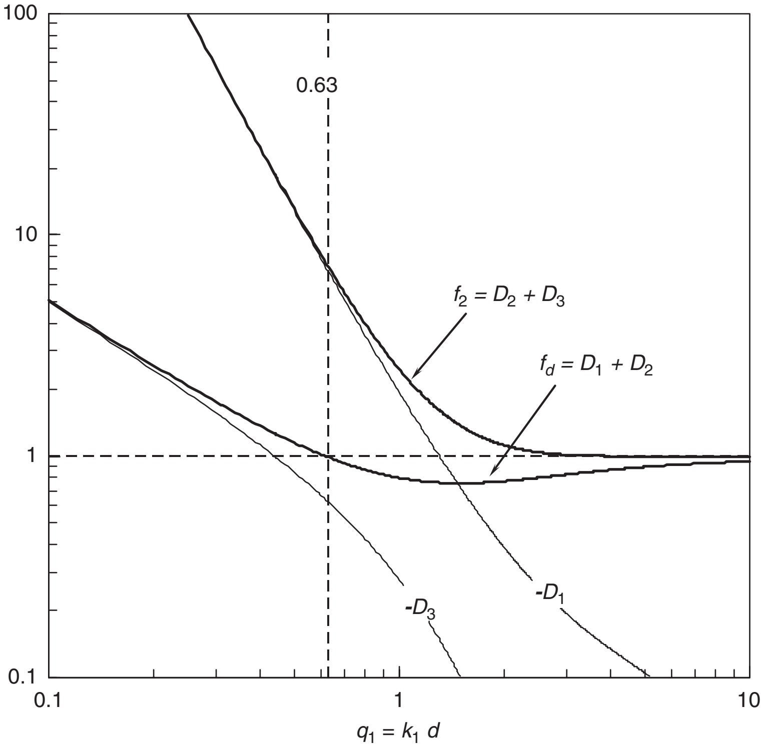

Fig. 3. Coefficients D_1, D_3, and depth factors $f_d = D_1 + D_2$ and $f_2 = D_2 + D_3$ versus q_1.

substantially, and so do $f_d = D_1 + D_2$ and $f_2 = D_2 + D_3$, as shown in Fig. 3. Clearly, f_2 over predicts the depth effects relative to f_d rather noticeably. Over the valid range $q_1 > q_{min} \approx 0.63$, $0.755 \leqslant f_d \leqslant 1$ whereas $1 \leqslant f_2 \leqslant 7$ approximately. These would suggest by way of $\lambda_3 = 3\mu^*$ that the Kriebel–Dawson formulation can give unrealistically large values of λ_3 at transitional water depths.

6. Verification and comparisons

6.1. Data and principal parameters

Of the two data sets analyzed in the following, the first comprises 9 h of measurements gathered during a severe storm in January, 1993 with a Marex radar from the Tern platform located in the northern North Sea in 167 m water depth. The second set represents 5 h of measurements gathered in January, 1998 with a Baylor wave staff from Meetpost Noordwijk in 18 m average water depth in the southern North Sea. Forristall (2000) elaborates the nature of the first data. The second data set is from Wave Crest Sensor Intercomparison Study (WACSIS). Further details on

WACSIS are given in Forristall et al. (2002). For brevity, these data will be referred to as TERN and WACSIS.

Physical specifics relevant to both sites and data, and the principal statistical and spectral parameters required by the models considered here are summarized in Tables 1–4. For simplicity, all results based on the Rayleigh law for scaled linear crests (r) and their groups are labeled as 'Ray'. Similarly, Forristall's 2D and 3D Weibull models and the Kriebel–Dawson model appropriate to nonlinear scaled crests (y) are labeled as F-2D, F-3D, and K–D, respectively, and all the present model predictions as T-R.

The statistics and spectral parameters summarized in the tables were derived from the analysis of each record treated as a whole, with the spectral estimates based on 600 degrees-of-freedom for TERN and 500 for WACSIS. The variations of $m_0^{1/2}$ observed over hourly segments in both records typically remain within ± 5–8% of the overall averages in Table 1. Thus, the sea states during both measurements appear to be fairly steady. The values of q_m and q_1 in Table 1 suggest that TERN is essentially a deep-water situation, whereas WACSIS represents a sea state in transitional waters. The parameters S_1, Ur, α and β for F-2D and F-3D are shown in Table 2.

The values of μ^* observed and implied by different models are summarized in Table 3. The values of $\mu^* = \lambda_3/3$ (data) in the first row simply follow from the

Table 1
Specifics and observed parameters of TERN and WACSIS

Description	TERN	WACSIS
Water depth d (m)	167	18
Record length T_R (s)	32,400	18,000
Sampling rate (Hz)	5.12	4
Wave count	3173	2668
$m_0^{1/2}$ (m)	3.0240	1.0379
λ_3	0.1738	0.2369
$T_m = 2\pi/\omega_m$ (s)	11.27	7.11
q_m	5.2939	1.4329
q_1	5.2939	1.5641

Table 2
Parameters in Forristall's models for TERN and WACSIS

Parameter	TERN		WACSIS	
	F-2D	F-3D	F-2D	F-3D
S_1	0.0610	0.0616	0.0526	0.0524
Ur	0.0026	0.0026	0.0943	0.0943
α	0.3715[a]	0.3696	0.3788[a]	0.3746
β	1.8683[a]	1.8883	1.8873[a]	1.8586

[a]Used in predictions of pdfs and epds by the Weibull model.

Table 3
Steepness parameter μ^* in various crest-height models

μ^*	(Model)	TERN	WACSIS
$\lambda_3/3$	(data)	0.0579	0.0790
μ_{F2}	(F-2D)	0.0793[a]	0.0979[a]
μ_{F3}	(F-3D)	0.0684	0.0918
μ_{KD}	(K–D)	0.0958[b]	0.1188[b]
$\mu_{ub} \approx \mu_m$	(upper bound)	0.0958[a]	0.0902

[a]Used in T-R model predictions.
[b]Used in K–D model predictions.

Table 4
Observed and band-pass spectral parameters

Parameter	TERN		WACSIS	
	Observed	Band-pass[a]	Observed	Band-pass[a]
ν	0.6287	0.1373	0.4896	0.1474
ω_m (rad/s)	0.5575	0.4785	0.8837	0.7333
ω_0 (rad/s)	0.6586	0.4830	0.9839	0.7472

[a]Used in all models for predicting group statistics.

estimates of λ_3 in Table 1. They are noticeably smaller than all model μ^* values. This is expected to be so because the sample estimates of λ_3 and thus μ^* (data) represent all waves, whereas the theoretical models and associated μ^* are biased toward large waves. The values $\mu^* = \mu_{F2}$ required for theoretical predictions are dictated by the F-2D model for use in T-R for both TERN and WACSIS. The values of $\mu^* = \mu_{\mathrm{KD}}$ for the K–D model are derived from Eq. (74). For TERN, $\mu_{\mathrm{KD}} = 0.0958$ is identical with μ_m, as it should be since K–D in deep water is based on the original narrow-band model (Tayfun, 1980) modified via series reversion. For WACSIS, $\mu_{\mathrm{KD}} = 0.1188$ is large due to the relatively large value of the depth-factor $f_2 = 1.318$ in this case. The band-pass values of ν, ω_m and ω_0 required in all model predictions of group statistics are given in Table 4.

The variations of $\mu_{\mathrm{ub}} \approx \mu_m$,μ_{F2}, $\mu_{1\mathrm{b}}$ and the actual $\mu^* = \lambda_3/3$ values estimated from 30-min segmental estimates of λ_3, m_0, ω_m and ν are shown in Fig. 4 for TERN. Clearly, these results confirm the validity of $\mu_{1\mathrm{b}}$ and $\mu_{\mathrm{ub}} \approx \mu_m = \mu_{\mathrm{KD}}$ as lower and upper bounds for the values observed. Further, it is seen that μ_{F2} approximates the observed peak values rather closely. It also correlates almost perfectly with μ_m, but is about 15–20% smaller than μ_m.

6.2. Miche limit and Ursell condition

The scatter of scaled wave heights $H/2m0^{1/2} \approx r$ and associated zero-up-crossing wave periods T/T_m scaled with the spectral 'mean' period $T_m = 2\pi/\omega_m$ is shown in

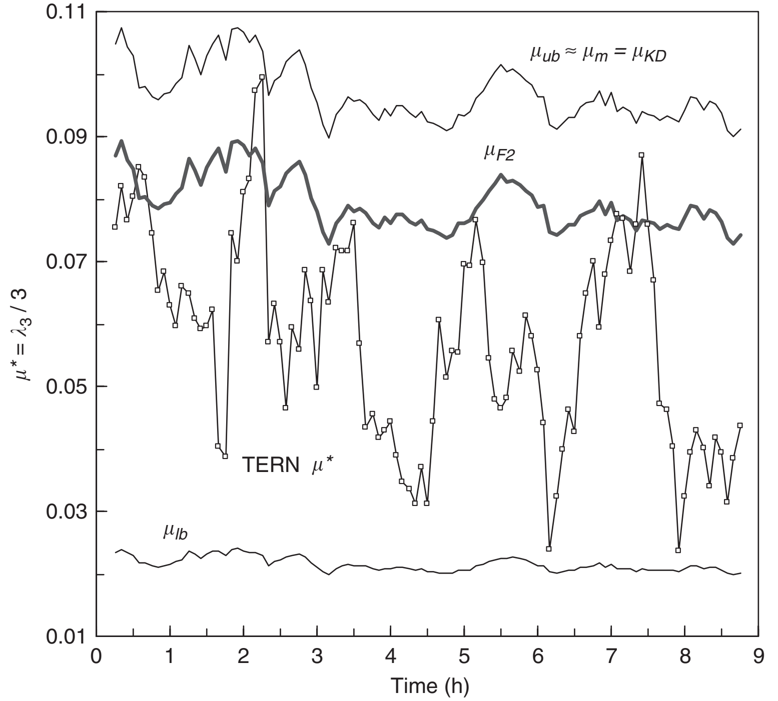

Fig. 4. Theoretical and observed μ^* from 30-min overlapping segments in TERN.

Fig. 5 for TERN and in Fig. 6 for WACSIS. The theoretical upper limit of Eq. (57) is indicated in both figures as 'Miche lim'. Evidently, the upper limit $r_{\max}$ in Eq. (59) should also be consistent with the Miche limit. For TERN, $r_{\max} = 22.08$ and lies far above the top range of Fig. 5. But, for WACSIS, $r_{\max} = 6.94$, as shown by the dashed horizontal line in Fig. 6. All considered, both figures demonstrate the efficacy of the Miche limit satisfactorily, except over rather low wave heights and periods.

The Ursell condition $Ur<2$ has relevance for WACSIS only, as TERN consists mostly of deep-water waves. The scatter of Ur versus $H/2m^{1/2}$ in WACSIS is plotted in Fig. 7, where it is seen that $Ur<0.41$ for all waves.

6.3. Validity of present model

The conditional mean $\langle r|\Lambda\rangle$ of $\underline{r}$, given $\Lambda = \{\underline{r} - \delta r/2 < r < \underline{r} + \delta r/2\}$, converges to $\underline{r}$ as $\delta r \to 0$. Assuming that Eqs. (26) and (27) are valid, then the ratios of the conditional means of y and y^-, given Λ and $\delta r << 1$, to $\underline{r}$ will admit the following approximations:

$$\frac{\langle y|\Lambda\rangle}{\underline{r}} \approx 1 + \frac{1}{2}\mu^* \underline{r}, \tag{76}$$

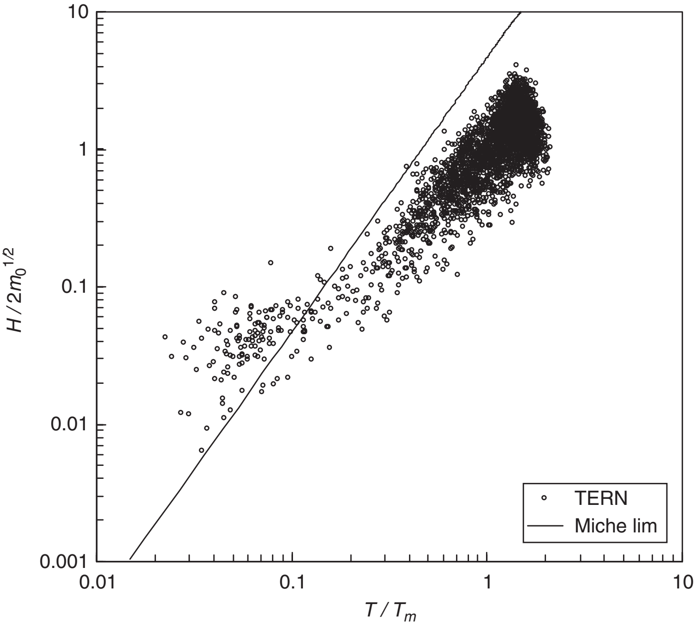

Fig. 5. Scatter of wave heights and periods in TERN.

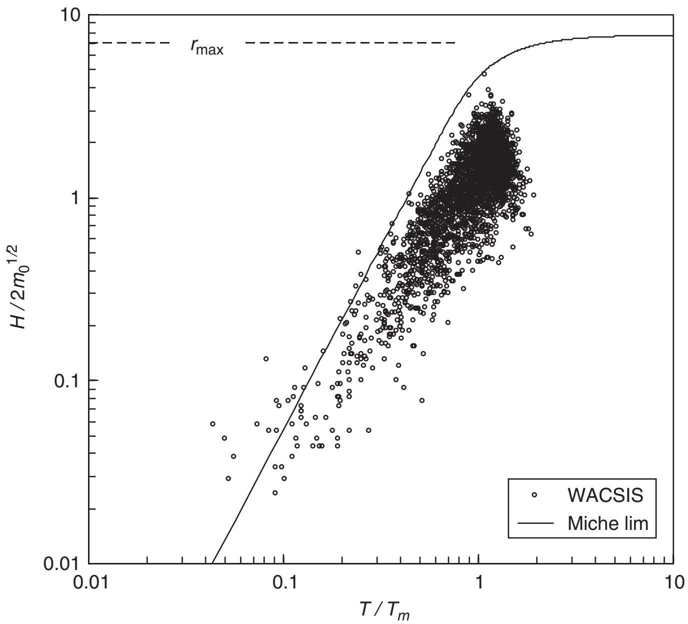

Fig. 6. Same as Fig. 5 but for WACSIS.

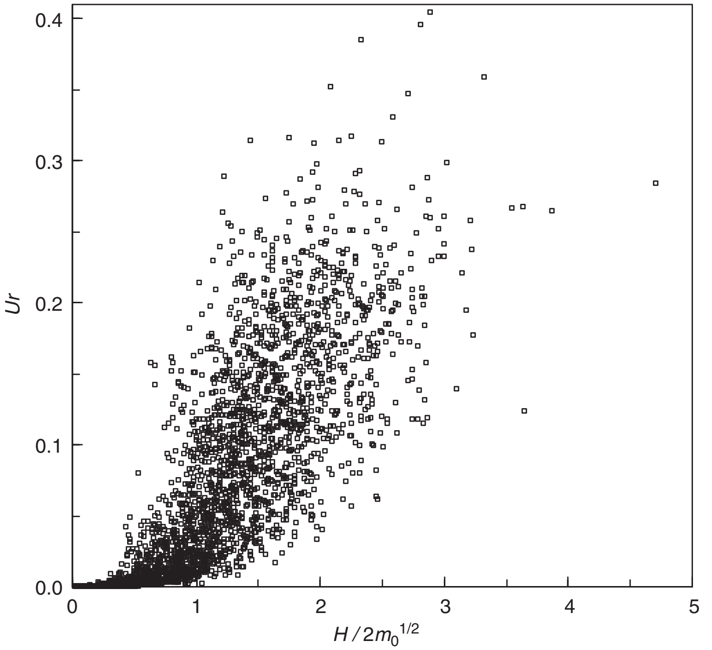

Fig. 7. Scatter of Ursell number Ur and wave heights in WACSIS.

$$\frac{\langle y^{-}|\Lambda\rangle}{\underline{r}} \approx 1-\frac{1}{2}\mu^{*}\,\underline{r}\,. \tag{77}$$

Simple as they are, these expressions provide a reasonably effective means of gauging the validity of the present nonlinear model relative to observational data. For TERN and WACSIS, the observed values of the left-hand side ratios in Eqs. (76) and (77) are plotted in Figs. 8 and 9, where $\delta r = 0.1$ uniformly for $0 < \underline{r} \leqslant 3.5$, and $\delta r > 0.1$ for $\underline{r} > 3.5$ as data become sparse toward the high-wave extreme. Linear regressions on the observed ratios and the theoretical predictions that follow from the right-hand sides of the same equations with $\mu_{F2} = 0.0793$ for TERN, and $\mu_{F2} = 0.0979$ for WACSIS from Table 3 are also shown in the same figures. The intercepts of the regression lines in both cases are specified as 1 to exclude the excess over very low waves. For the most part, the theoretical predictions in both cases approximate the regression lines closely and describe the observed data reasonably well. Large deviations from the models do appear over very high waves as the observed data become sparse and yield highly variable estimates.

It should be noted that for the upper bound $\mu_{ub} \approx \mu_m = 0.0958$ in TERN, the theoretically predicted ratios are given by $1 \pm 0.0479\,\underline{r}$. Although these are not shown in Fig. 8 for clarity of presentation, it is evident that they compare with the regressions lines $1 \pm 0.0454\,\underline{r}$ more favorably than $1 \pm 0.0397\,\underline{r}$ based on $\mu_{F2} = 0.0793$. Further, both Figs. 8 and 9 show that for any $\underline{r}$, crest and trough

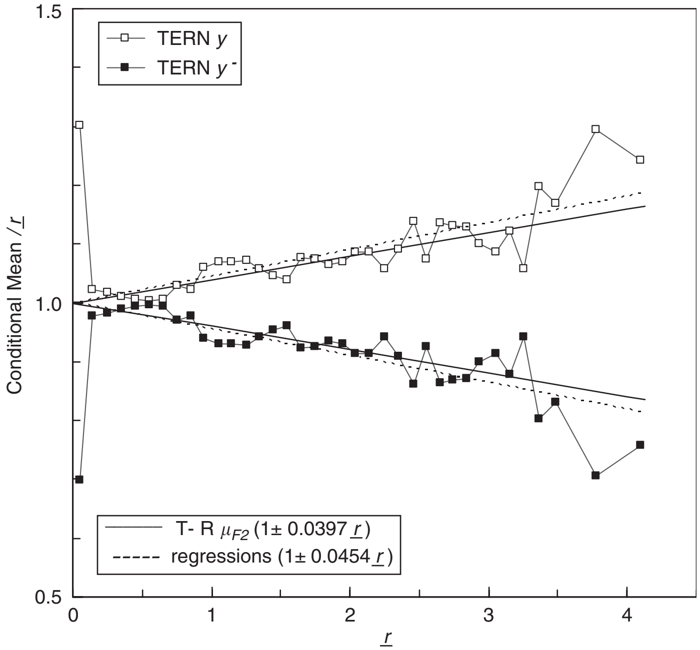

Fig. 8. Theoretical versus observed conditional moments of crests and troughs in TERN.

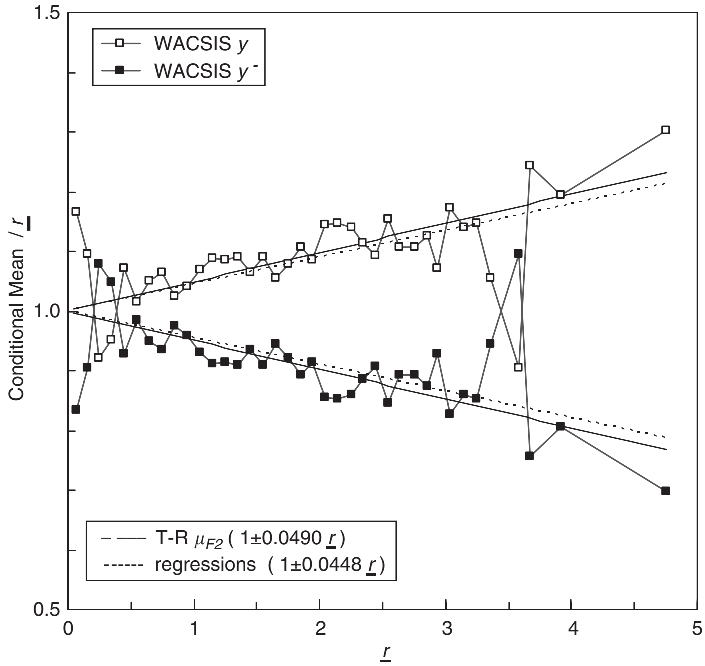

Fig. 9. Same as Fig. 8 but for WACSIS.

heights form nearly perfect mirror images of one another with respect to a horizontal line drawn through the intercept at 1. This confirms the expectation that on average, second-order nonlinearities shift wave crests and troughs upward through the same incremental distance.

6.4. *Comparisons of crest-height pdfs*

The observed pdfs in TERN and WACSIS are shown in Figs. 10 and 11 in comparisons with the theoretical pdfs from Ray, F-2D, K–D and T-R . In either case, it is observed that F-2D and T-R describe the data fairly well for $y > 1.25$. The theoretical pdf from T-R based on the upper bound $\mu_m = 0.0958$ is also shown in Fig. 10 for TERN. The latter pdf differs very little from the T-R pdf based on $\mu_{F2} = 0.0793$. However, the K–D pdfs overestimate the data noticeably for $y > 2.5$–3 in both cases.

For $y < 1.25$, all model predictions compare poorly with the data. The waves for which $y < 1.25$ comprise about 50% of the whole wave count in both cases. The observed pdfs typically display a bimodal or doubly peaked structure previously alluded to in the introduction. This appears more pronounced in TERN with a wider spectral bandwidth and far more energetic waves than WACSIS. The initial peak is indicative of an excess in crest heights over low waves. Simulations with linear and nonlinear 2D waves showed that such excesses arise from data with wide-band spectral characteristics. TERN and WACSIS represent wide-band waves, with the observed spectral densities in both cases decaying as ω^{-4} for $\omega > 4\omega_p$ approximately.

6.5. *Comparisons of epds and conditional means*

The observed epds and conditional means $y_{1/n}$ are shown in Figs. 12 and 13 for TERN, and in Figs. 14 and 15 for WACSIS. The theoretical predictions from all models are included in these figures, except for $y_{1/n}$ from K–D. The predictions of T-R based on the upper bound $\mu_m = 0.0958$ are also in Figs. 12 and 13 for TERN for comparison. The epd plots in Figs. 12 and 14 have a semi-logarithmic form, emphasizing the data trends toward the high-wave extreme. Clearly, the F-2D and T-R models describe the data fairly well in all cases, whereas the comparisons in both Figs. 12 and 14 indicate that the K–D model does rather poorly. In general, T-R predictions based on μ_{F2} match the observed trends somewhat better over the range of high waves where the F-2D model has a tendency to under predict the data slightly. Also, if the K–D model were modified in the manner described in Forristall (2000) and Forristall and Prevosto (2002), the resulting predictions would improve for TERN noticeably, but they would become still worse for WACSIS. A clear discrepancy between all model predictions and data trends does arise over the very extreme tail where the data are sparse and display a systematic bias for rather large values. This is most noticeable in Figs. 14 and 15 for WACSIS, which contains an extremely large crest corresponding to the largest outlier in Fig. 14.

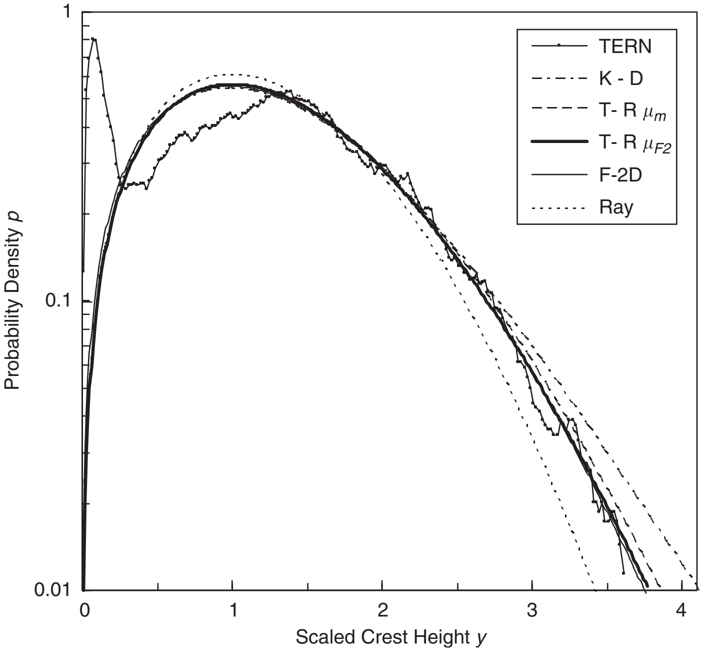

Fig. 10. Theoretical versus observed pdfs in TERN.

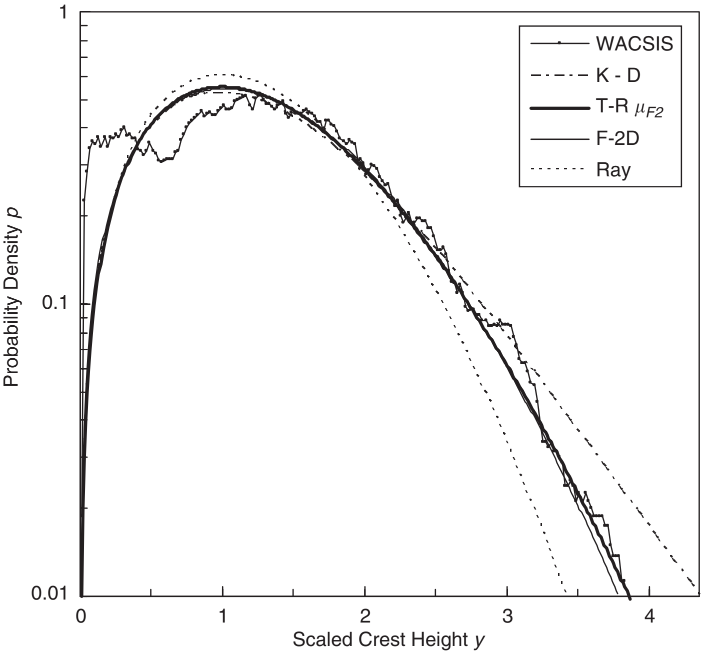

Fig. 11. Same as Fig. 10 but for WACSIS.

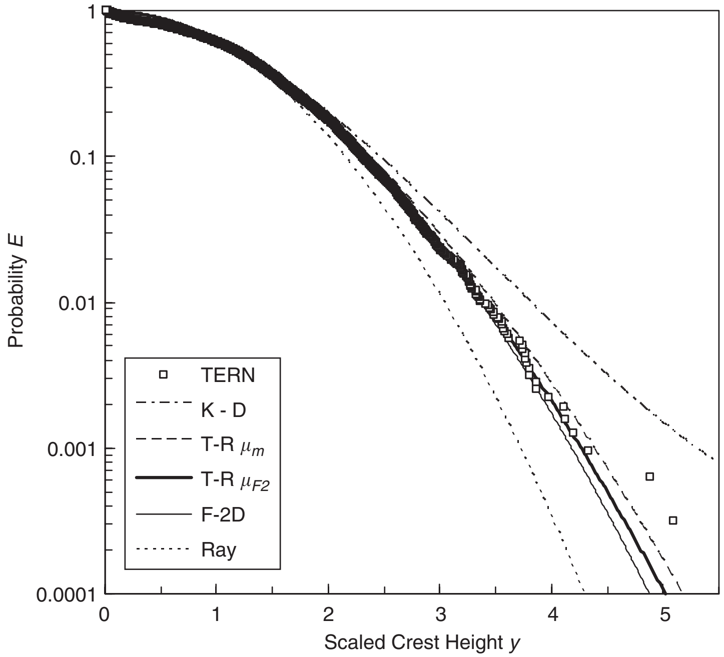

Fig. 12. Theoretical versus observed epds in TERN.

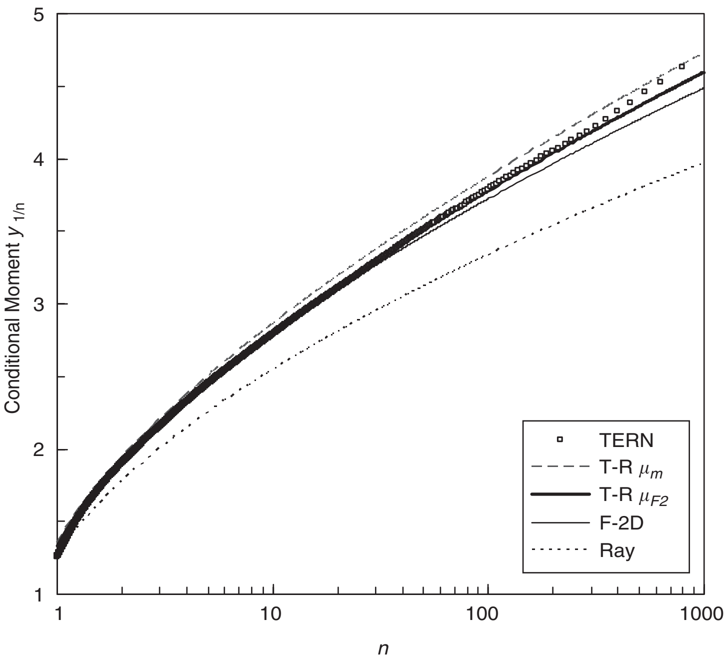

Fig. 13. Theoretical versus observed conditional moments $y_{1/n}$ in TERN.

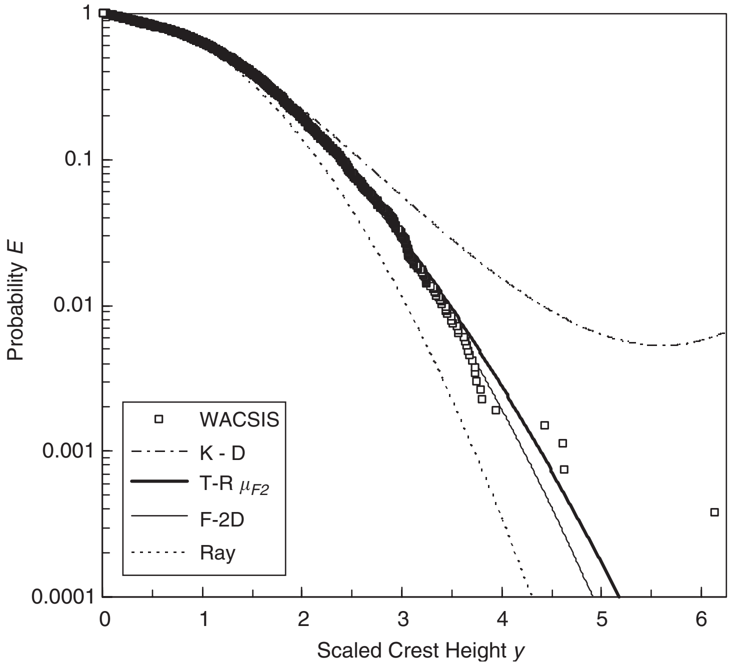

Fig. 14. Same as Fig. 12 but for WACSIS.

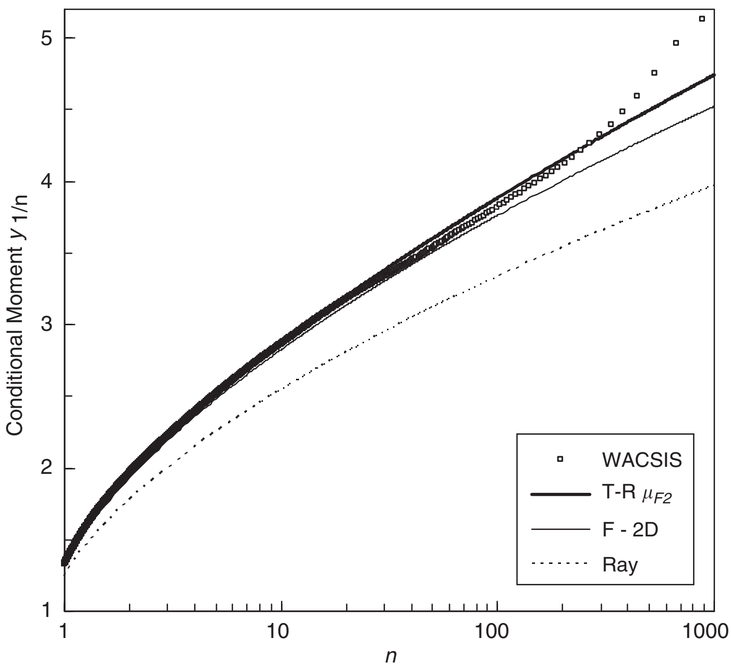

Fig. 15. Same as Fig. 13 but for WACSIS.

6.6. Statistics of crest groups

The total number of up-crossings of level y in a record of length T_R is given by $N_y T_R$. The observed values of $N_y T_R$ and the corresponding theoretical predictions Ray, T-R and K–D are shown in Figs. 16 and 17 for TERN and WACSIS, respectively. Similar comparisons between the observed G_y, H_y and the corresponding theoretical predictions are likewise given in Figs. 18 and 19 for G_y, and in Figs. 20 and 21 for H_y. The observed statistics are based on threshold levels at uniform increments of $\Delta y = 0.2$. In all cases, the general trend of the observed statistics are represented quite favorably by the T-R model predictions based on μ_{F2} for both TERN and WACSIS. The T-R model predictions based on μ_m for TERN describe the data reasonably well also, but not always as consistently as the T-R predictions based on μ_{F2} do, for example, as in Figs. 16 and 18. All models yield similar predictions that compare favorably with the data for $y < 2$ approximately. But, Ray and K–D models deviate progressively from the observed trends at higher threshold levels. However, some discrepancies between the observed data and all models do appear also when $y < 2$. For example, in Fig. 16 for TERN, all models systematically underestimate the number of actual up-crossings. Arguably, this can be explained in terms of the wide-band or simply 'noisy' nature of wave envelopes, and thus their tendency to 'split' wave groups (Masson and Chandler, 1993). In nonlinear waves with sharper higher crests and flatter shallower troughs, splitting of wave-crest groups by the wave envelope is likely to occur more frequently. Band-passing the spectral density over ($0.5\omega_{\mathrm{p}}$, $1.5\omega_{\mathrm{p}}$) does help reduce splitting, but it does not entirely eliminate it in all cases. Evidently, the discrepancies in $N_y T_R$ of Fig. 16 due to splitting also carry over to Figs. 18 and 20 for TERN, but they do not appear to affect the comparisons of G_y and H_y to the same extent as in Fig. 16.

7. Conclusions

The effects of nonlinearities on the statistics of wave crests and their groups were considered, using the continuous envelope approach and a specific second-order nonlinear model appropriate to large waves. The model is simple, and yet quite effective in that it allows all nonlinear crest-height and crest-group statistics to be predicted by way of a quadratic transformation of well-known results on linear waves. If the key parameter representing wave steepness and thus nonlinearity is specified in accord with Forristall's (2000) simulations, then the proposed model and the theoretical expressions derived from it describe the observed statistics quite well over high waves in both deep and transitional water depths. Apparently, the upper-bound form of the steepness parameter derived in this study presents a somewhat simpler alternative in deep water, and leads to predictions that also compare favorably with the observed data.

The model previously proposed by Kriebel and Dawson (1991, 1993) describes the observed statistics reasonably well over low waves, as all other linear and nonlinear models do, but it does rather poorly over high waves. In deep water, this is largely

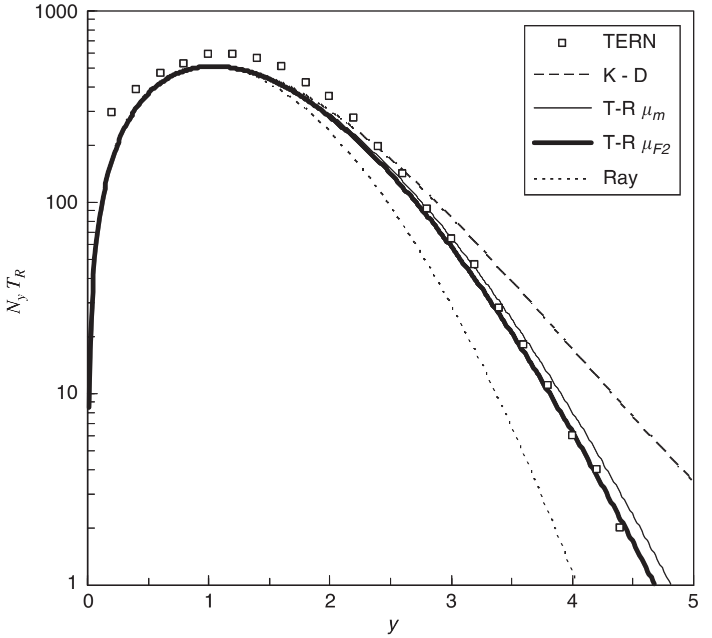

Fig. 16. Total number of up-crossings: model predictions versus TERN.

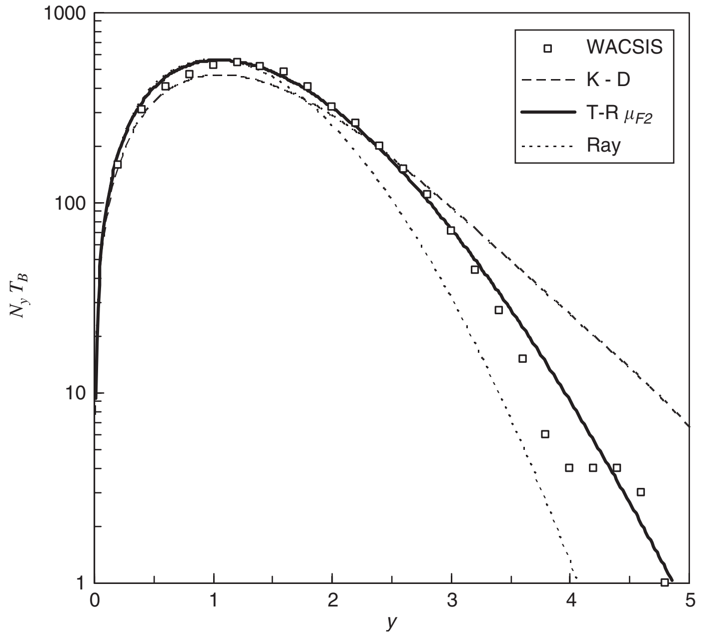

Fig. 17. Same as Fig. 16 but for WACSIS.

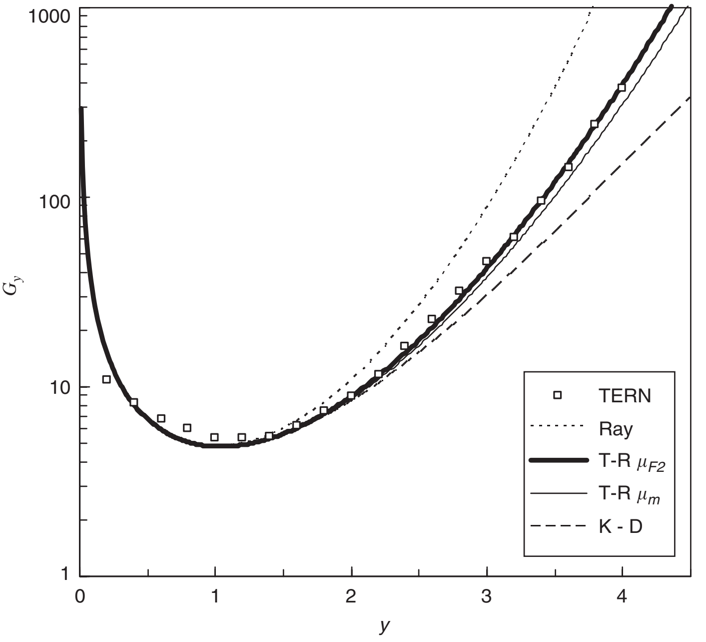

Fig. 18. Mean run lengths corresponding to Fig. 16: model predictions versus TERN.

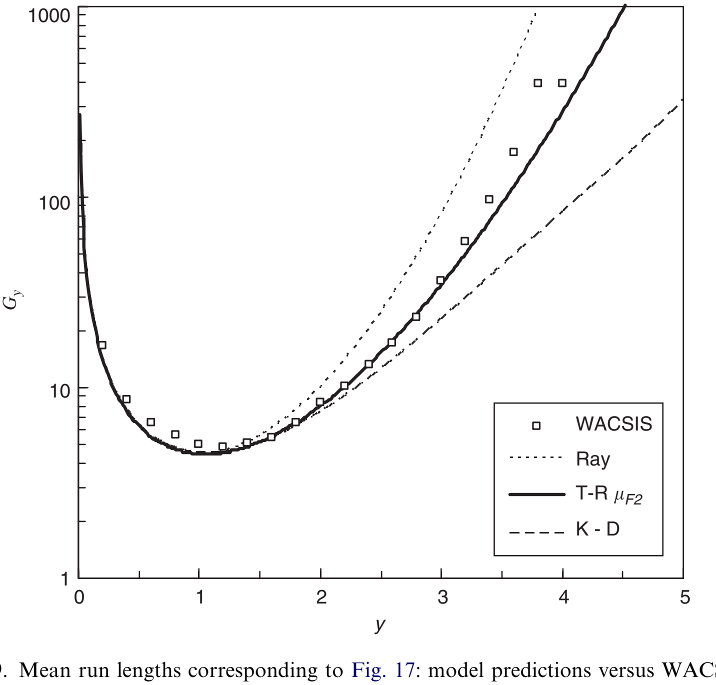

Fig. 19. Mean run lengths corresponding to Fig. 17: model predictions versus WACSIS.

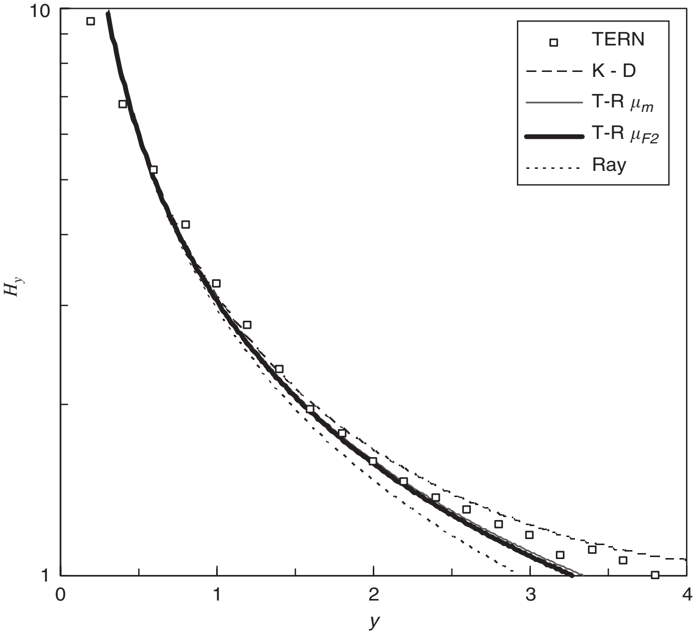

Fig. 20. Mean length of high runs corresponding to Fig. 18: model predictions versus TERN.

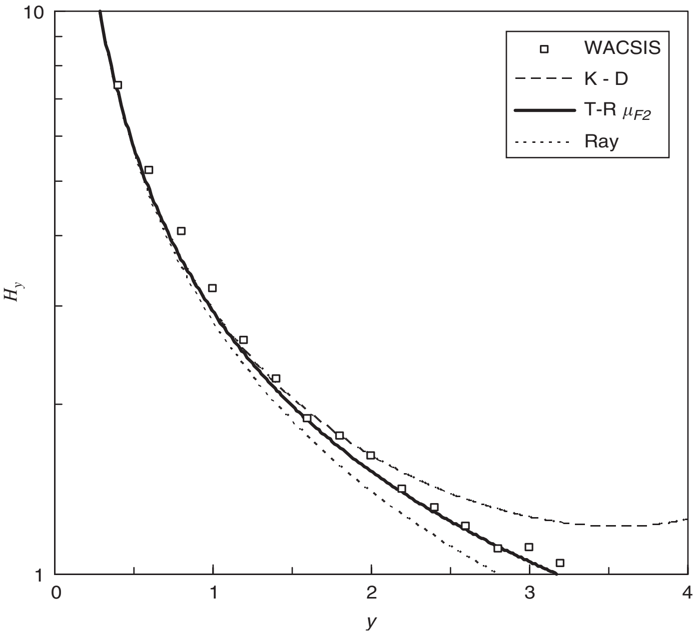

Fig. 21. Mean length of high runs corresponding to Fig. 19: model predictions versus WACSIS.

because of errors arising from the series-reversion employed in their derivations. At transitional depths, additional errors arise from representing the finite-depth effects in analogy with the deterministic Stokes theory. This approach does not lead to a correct representation of irregular waves in transitional waters.

Acknowledgments

The author acknowledges with much appreciation that George Z. Forristall, Forristall Ocean Engineering, Inc., Camden, ME, USA, and Francisco Fedele, Goddard Earth Sciences Technology Center, NASA Goddard Space Flight Center, Greenbelt, MD, USA, provided a variety of useful comments on an earlier draft of this paper. The author also acknowledges, certainly with no less appreciation, that George Z. Forristall and Marc Prevosto, Ifremer, France, provided the author with the data utilized in this study.

References

Abramowitz, M., Stegun, I.A., 1968. Handbook of Mathematical Functions. Dover Publications, New York, pp. 944–945.

Arena, F., Fedele, F., 2002. A family of narrow-band nonlinear stochastic processes for the mechanics of sea waves. European Journal of Mechanics B/Fluids 21, 125–137.

Arhan, M., Plaisted, R.O., 1981. Nonlinear deformation of sea-wave profiles in intermediate and shallow water. Oceanologica Acta 4, 107–115.

Askar, H., Tayfun, M.A., 1999. Excedance distribution of large wave amplitudes. Kuwait University Journal of Science and Engineering 26 (2), 225–238.

Battjes, J.A., Van Vledder, G.Ph., 1984. Verification of Kimura's theory for wave group statistics. Proceedings, 19th International Coastal Engineering Conference, American Society of Civil Engineers, pp. 642–648.

Boccotti, P., 2000. Wave Mechanics for Ocean Engineering. Elsevier Science, New York, pp. 1–496.

Butler, R.W., Machado, U.B., Rychlik, I., 2003. Distribution of wave crests in non-Gaussian seas. Proceedings, 13th International Offshore and Polar Engineering Conference, International Society of Offshore and Polar Engineers, pp. 71–78.

Dawson, T.H., 2004. Stokes correction for nonlinearity of wave crests in heavy seas. Journal of Waterway, Port, Coastal and Ocean Engineering, American Society of Civil Engineers 130 (1), 39–44.

Dawson, T.H., Kriebel, D.L., Wallendorf, L.A., 1991. Experimental study of wave groups in deep-water random waves. Applied Ocean Research 13 (3), 116–131.

Dawson, T.H., Kriebel, D.L., Wallendorf, L.A., 1996. Markov description of wave crest statistics. Journal of Offshore Mechanics and Arctic Engineering, American Society of Mechanical Engineers 118, 37–45.

Dean, R.G., Dalrymple, R.A., 1998. Water Wave Mechanics for Engineers and Scientists. World Scientific, Singapore.

Doering, J.C., Donelan, M.A., 1993. The joint distribution of heights and periods of shoaling waves. Journal of Geophysical Research 98 (C7), 12543–12555.

Fedele, F., 2004. The occurrence of extreme crests and the nonlinear wave-wave interaction in random seas. Proceedings, 14th International Offshore and Polar Engineering Conference, vol. 3, International Society of Offshore and Polar Engineers, pp. 55–62.

Fedele, F., Arena, F., 2005. Weakly nonlinear statistics of high random waves. Physics of Fluids 17 (1), 1–10 (Paper no. 026601).

Forristall, G.Z., 2000. Wave crest distributions: observations and second-order theory. Journal of Physical Oceanography 30 (8), 1931–1943.

Forristall, G.Z., Krogstad, H.E., Taylor, P.H., Barstow, S.S., Prevosto, M., Tromans, P., 2002. Wave crest sensor intercomparison study: an overview of WACSIS. Proceedings, 21st International Conference on Offshore Mechanics and Arctic Engineering, American Society of Mechanical Engineers, Paper no. OMAE2002-28438, pp. 1–11.

Goda, Y., 1976. On wave groups. Proceedings, Behavior of Offshore Structures, Trondheim, Norway, pp.115–128.

Goda, Y., 2000. Random Seas and Design of Maritime Structures. World Scientific, Singapore.

Guizhen, Z., Xuren, H., Delun, X., 2004. A discrete correction scheme for envelope approach of wave group statistics. Coastal Engineering 50, 225–230.

Huang, E.N., Tung, C.-C., Lai, J.L., 1985. A note on the statistics of threshold crossing for a nonlinear wave field. Ocean Engineering 12 (4), 363–368.

Huang, N.E., Long, S.R., Tung, C.C., Yuan, L., Bliven, F., 1983. A non-Gaussian model for surface elevation of nonlinear random wave fields. Journal of Geophysical Research 88, 7597–7606.

Kimura, A., 1980. Statistical properties of random wave groups. Proceedings, 17th International Coastal Engineering Conference, American Society of Civil Engineers, pp. 2955–2973.

Kriebel, D.L., Dawson, T.H., 1991. Nonlinear effects on wave groups in random seas. Journal of Offshore Mechanics and Arctic Engineering. American Society of Mechanical Engineers 113, 142–147.

Kriebel, D.L., Dawson, T.H., 1993. Nonlinearity in crest height statistics. Proceedings, 2nd International Conference on Wave Measurement and Analysis, American Society of Engineers, pp. 61–75.

Longuet-Higgins, M.S., 1958. On the intervals between zeros of a random function. Proceedings of the Royal Society of London A 246, 99–118.

Longuet-Higgins, M.S., 1963. The effect of nonlinearities on statistical distributions in the theory of sea waves. Journal of Fluid Mechanics 9, 193–217.

Longuet-Higgins, M.S., 1964. Modified distributions for slightly nonlinear variables. Radio Science Journal of Research 68D (9), 1049–1062.

Longuet-Higgins, M.S., 1984. Statistical properties of wave groups in a random sea state. Philosophical Transactions of Royal Society of London A 312, 219–250.

Marthinsen, T., Winterstein, S.R., 1992. On the skewness of random surface waves. Proceedings, 2nd International Offshore and Polar Engineering Conference, International Society of Offshore and Polar Engineers, pp. 472–478.

Masson, D.E., Chandler, P., 1993. Wave groups: a closer look at spectral methods. Coastal Engineering 20, 249–275.

Miche, R., 1944. Mouvements ondulatoires de la mer en profoundeur constante ou decroissante. Annales des Ponts et Chaussees 121, 285–318.

Ochi, M.K., Sahinoglou, I.I., 1989. Stochastic characteristics of wave groups in random seas. Applied Ocean Research 11, 112–118.

Peregrine, D.H., 1972. Equations for water waves and the approximation behind them. In: Mayer, R.E. (Ed.), Waves on Beaches and Resulting Sediment Transport. Academic Press, New York, pp. 95–121.

Prevosto, M., Forristall, G.Z., 2002. Statistics of wave crests from models vs. measurements. Proceedings, 21st International Conference on Offshore Mechanics and Arctic Engineering, American Society of Mechanical Engineers, Paper no. OMAE2002-28443, pp. 1–11.

Prevosto, M., Krogstad, H.E., Robin, A., 2000. Probability distributions for maximum wave and crest heights. Coastal Engineering 40, 329–360.

Rice, S.O., 1958. Distribution of the duration of fades in radio transmission—Gaussian noise model. Bell System Technology Journal 37, 581–635.

Sharma, J.N., Dean, R.G., 1979. Development and evaluation of a procedure for simulating a random directional second order sea surface and associated wave forces. Ocean Engineering Report 20, University of Delaware, Newark.

Stansell, P., 2004. Distributions of freak wave heights measured in the North Sea. Applied Ocean Research 26, 35–48.

Stansell, P., Wolfram, J., Linfoot, B., 2002. Statistics of wave groups in the northern North Sea: comparisons between time series and spectral predictions. Applied Ocean Research 24, 91–106.

Tayfun, M.A., 1980. Narrow-band nonlinear sea waves. Journal of Geophysical Research, American Geophysical Union 85 (3), 1548–1952.

Tayfun, M.A., 1986. On narrow-band representation of ocean waves 1. Theory. Journal of Geophysical Research, American Geophysical Union 91 (C6), 7743–7752.

Tayfun, M.A., 1994. Distributions of envelope and phase in weakly nonlinear random waves. Journal of Engineering Mechanics, American Society of Civil Engineers 120 (4), 1009–1025.

Tayfun, M.A., 2004. Statistics of wave crests in storms. Journal of Waterway, Port, Coastal and Ocean Engineering, American Society of Civil Engineers 130 (4), 155–161.

Tayfun, M.A., Al-Humoud, J., 2002. Least upper bound distribution for nonlinear wave crests. Journal of Waterway, Port, Coastal and Ocean Engineering, American Society of Civil Engineers 128 (4), 144–151.

Tromans, P.S., Taylor, P.H., 1998. The shapes, histories and statistics of non-linear wave crests in random seas. Proceedings, 17th International Conference on Offshore Mechanics and Arctic Engineering, American Society of Mechanical Engineers, Paper no. OMAE98-1206, pp. 1–6.

Vanmarcke, E.H., 1975. On the distribution of the first-passage time for normal stationary random processes. Journal of Applied Mechanics, American Society of Mechanical Engineers 42, 215–220.

Wist, H.T., Myrhaug, D., Rue, H., 2002. Nonlinearity in successive wave crest heights and successive wave trough depths for second-order nonlinear waves. Journal of Ship Research 46 (3), 175–185.